

## Experimental Study on Preceding Viscoelastic Strain Disturbances

—An Inverse Problem in Dynamic Fracture—

By

Akira KOBAYASHI and Nobuo OHTANI

*Summary:* The experimental study on the inverse problem in dynamic fracture in a viscoelastic solid is achieved. The preceding wavy strain disturbances ahead of a running crack are observed through high speed Schlieren photography, showing a possibility of intermittent crack propagation. It is found that the effect of breaking stress is predominant in these wavy strain disturbances in a viscoelastic solid, while the strain rate effects little contribute on the very disturbances.

### INTRODUCTION

The study on the stress pulses or strain pulses leading to the dynamic fracture is now more than a century old. As is well-known, the earliest work concerning the relation between the propagation of elastic pulses in solids and the resulting brittle fracture was done by John Hopkinson [1] in 1872. He published a paper on the strength of steel wires subjected to tensile impact. Afterwards, in 1914, John Hopkinson's son Bertram [2] described about the spalls produced in steel plates as a result of explosive detonation on the opposite side of a plate. After World War II, extensive literature in this connection has been accumulated [3-4].

On the other hand, there also exists the **inverse** problem, that is, the stress pulses produced by the brittle fracture, which may be considered as one example of acoustic stress wave emission. This problem is much younger compared with that of previous conventional dynamic fracture due to the stress wave propagation. The first paper concerning this was appeared by Miklowitz [5] in 1952, as a discussion of stress waves generated in case of a brittle rod fracture in tension. Miklowitz noticed the fact that a second break frequently occurs at some other point along the rod subjected to simple tension. He predicted the above phenomenon might be due to the interaction between the reflection of compressive stress pulses at the ends of the rod and the flexural stress pulses, generated as a result of fracture initiating from the surface of the rod, propagating outwards cylindrically, therefore, a couple is built up on the fracture surface. No experimental verification was made until Phillips' experiment [6] done for circular glass

rods in 1970. Earlier in 1967, Tsai and Kolsky [7] studied the stress pulses produced in case of a Hertzian fracture caused by the steel ball impact on glass block, and Tsai [8] presented more detailed work later. Kolsky [9] also described about "The stress pulses propagated as a result of the rapid growth of brittle fracture", in 1973. Anyway, further effort will be much more required in this connection.

All the materials described above are concerned with elastic brittle ones such as glass, and no viscoelastic materials are of interest. The present paper reports on the visual observation of viscoelastic strain disturbances running ahead of a propagating crack due to the dynamic fracture in a viscoelastic solid through high speed Schlieren photography, of which details will be described in what follows. This is one example of the **inverse** problem in a viscoelastic solid.

### EXPERIMENTAL

A Cranz-Schardin type multiple spark camera, Chronolite, made by Impulsphysik GmbH, Hamburg West Germany, was employed to take Schlieren photographs for rapid events in the present study. Owing to the de-ionization time of the plasma between the electrodes it is not possible to realize very high taking rates in a single spark gap. In a photographic arrangement devised by Cranz-Schardin the single sparks are generated in separate spark gaps. This method can achieve considerably higher flashing rates as compared to the possible repetition rate of a single spark gap. Fig. 1 shows the light paths of the illumination sparks and the frame separation by means of prisms. The spark head and taking camera can also be arranged opposite each other. Turning now to further technical details in the followings.

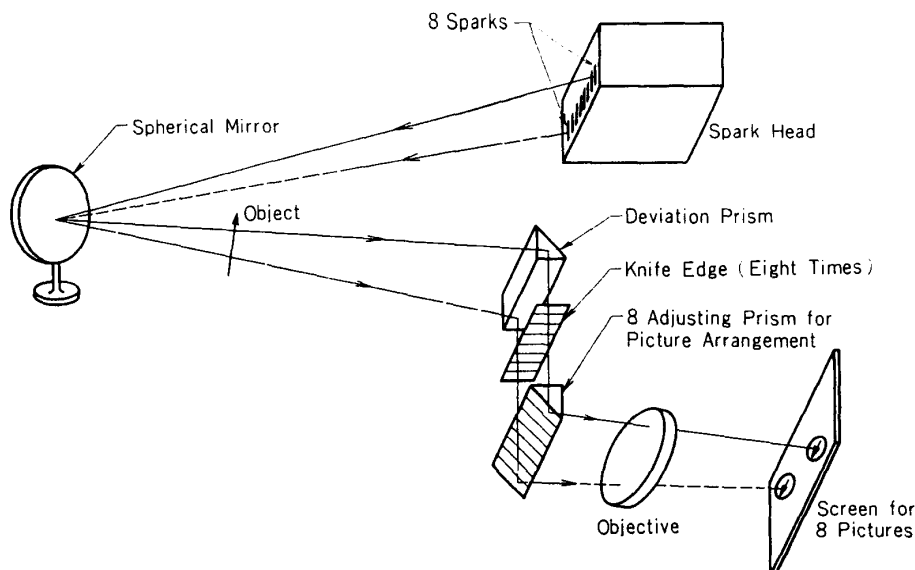


FIG. 1 Cranz-Schardin type multiple spark camera: Diagram showing the optical path and frame separation

### Basic Electronic Equipment

The basic electronic equipment is mainly transistorized and portable. In addition to the adjustable high voltage supply for the spark capacitors it contains the impulse generator, with time interval variable from 1 microsecond to 1 second. The preselected time interval is the same for all eight pictures. An external trigger pulse, shown in Fig. 2, starts the impulse generator, which supplies spike impulses of 40 nanosecond half width.

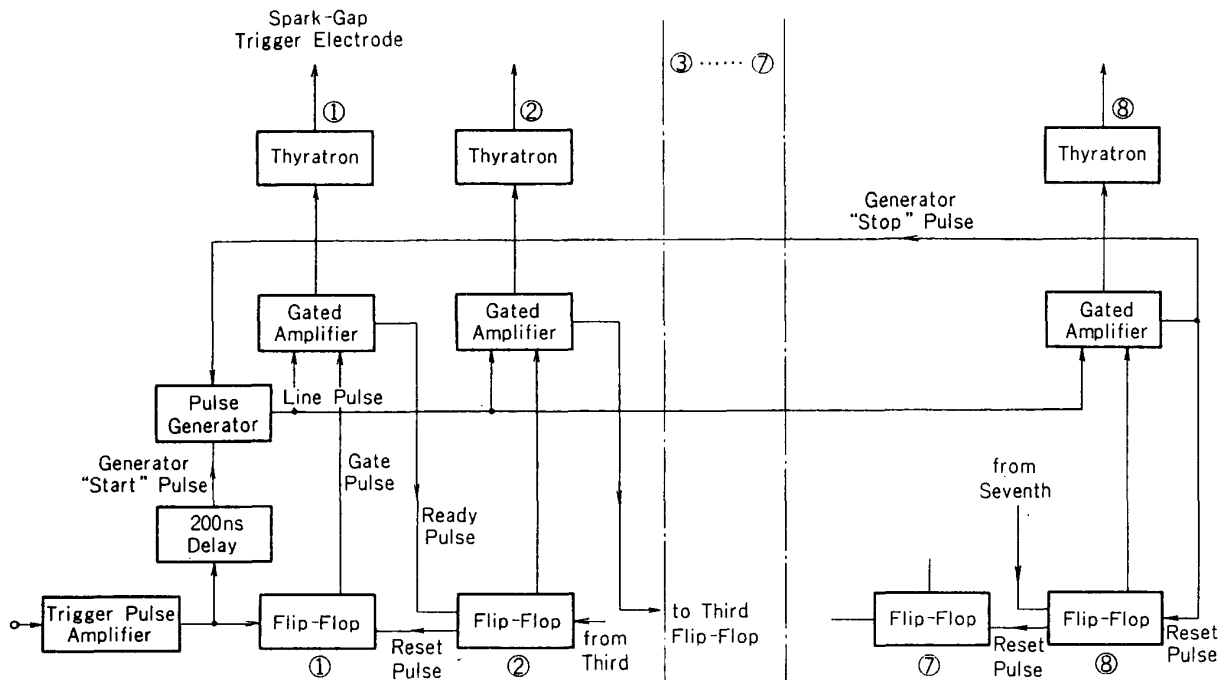


FIG. 2 Block diagram of the time control

Simultaneously, the first flipflop in the shift register of an eight-section circuit is triggered. This, in turn, opens a gate amplifier through which the first pulse from the impulse generator triggers the first thyatron. In addition to the trigger pulse for the thyatron the amplifier sends another starting impulse to the following flipflop. Consequently, the trigger sequence described is repeated at equal intervals in accordance with the pre-set time schedule. The thyratrons, via impulse transformers, trigger the corresponding spark gaps. After the eight circuits have been triggered, a final pulse stops the impulse generator. Also, the eight flipflops are pulsed back to the reset condition immediately after their switching action. Following each series, the equipment is ready to start again as soon as the spark gap capacitors are recharged in approximately 3 seconds.

### Spark Gap Unit

The eight spark gap unit comprises eight three-electrode air spark gaps. The third electrode is the trigger electrode and is mounted eccentrically with respect to the spark center. The spark gaps are triggered directly and not

by the more usual, series-connected spark gap. The resulting advantages are: low time jitter of about 30 nanoseconds, no additional losses of energy, extremely low inductance discharge path and therefore very short flash duration times of under 100 nanoseconds. A capacitor of 10 nF charged to 5 kV gives a discharge of 0.063 Ws, which experience shows is adequate for shadowgraphy and Schlieren photography.

The spark gaps are arranged in one vertical row and spaced 9 mm apart. With an object distance of 3 to 5 m the vertical parallax is hardly noticeable, because of the small spark separation, while there is no horizontal parallax. The small spark dimensions of  $2 \times 0.5$  mm make a pinhole mask unnecessary. An auxiliary continuous light source with eight miniature lamps can be plugged in for alignment and adjustment. In principle it is possible to place the entire spark gap assembly in a rare gas environment, which results in a corresponding light increase. The order of the spark sequence can be arbitrarily changed by means of plug-in connectors, which is useful for varying the spark unit.

The tungsten electrodes of the spark gaps are individually adjustable so that for any selected voltage all spark gaps have exactly the same breakdown voltage, ensuring that only triggered sparks are fired. Particularly in this spark head, Teflon has proved to be excellent insulation material.

### Camera Head

The receiving head of the camera comprises as essential components: the rotating shutter, a reflex prism common for all eight pictures, eight knife edges located in the spark image plane and adjustable in unison, eight adjustable reflex prisms for image separation, and an achromatic lens as photographic objective as shown in Fig. 3. The arrangement of the spark gaps and the spark images in one row with small separation permits a simple construction of the components in the camera head. The use of a rotating slit shutter with synchronization contact for event triggering permits operation in moderately illuminated rooms. The utilization of a common objective lens for all eight pictures provides for simple focusing to any object

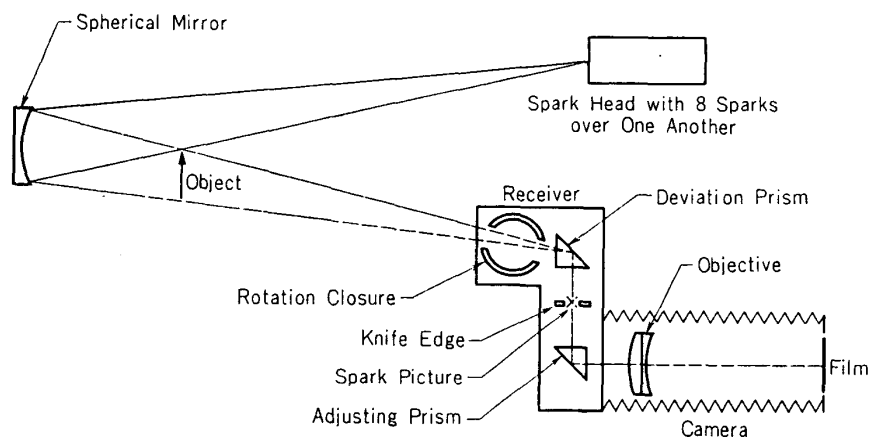


FIG. 3 Camera head mechanism

distance by sliding the back of the camera toward or away from the lens. Optimum utilization of the  $9 \times 12$  cm film area can be achieved with the aid of the adjustable prisms. Provision is made for the use of polaroid material, plates or cut film.

### Test Specimen

Polymethyl methacrylate (PMMA) specimens were cut out of Sumipex virgin sheets, produced by Sumitomo Chemical Company, Japan, of which dimensions are as shown in Fig. 4. Notice two kinds of initial notch radius, 2.5 mm and 0.02 mm, were prepared so as to obtain different breaking stresses. Du Pont No. 4817 conductive silver coating material is placed just in contact with the initiation notch for triggering purpose.

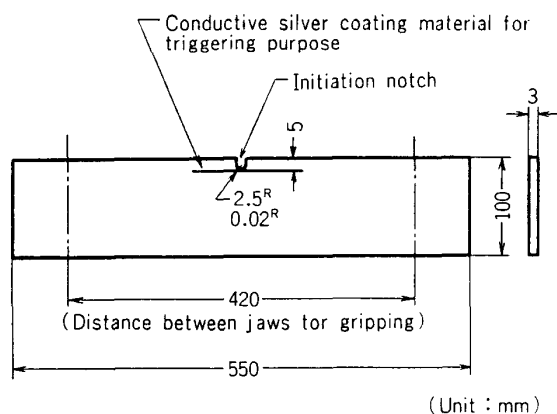


FIG. 4 PMMA specimen dimensions

### Experimental Conditions and Results

An Instron type tensile tester, UTM-1, of Toyo-Baldwin make was used to initiate a crack on the specimen with different constant strain rates. The breaking load was measured by a load cell. The test condition for Schlieren photography is shown in Table 1.

TABLE 1 Test condition

Spark head pressure	2.6 Kg/cm <sup>2</sup>	Argon was used
Spark head voltage	2.3 KV	
Time interval between pictures	25 microseconds	
Test temperature	approx. 15°C	

### Experimental Results

The Schlieren photographs thus taken are shown in Figs. 5 to 7. These experimental results are also tabulated as shown in Table 2.

TABLE 2 Summary of experimental results

Specimen No.	Initiation crack tip radius $\rho$	Applied strain rate $\dot{\epsilon}$	Breaking stress $\sigma_b$
3	2.5 mm	$1.93 \times 10^{-2}/S$	3.6 Kg/mm <sup>2</sup>
13	0.02 mm	$7.93 \times 10^{-5}/S$	1.8 Kg/mm <sup>2</sup>
14	2.5 mm	$7.93 \times 10^{-5}/S$	4.3 Kg/mm <sup>2</sup>

Among the above experimental results, those for No. 3 specimen are partly quoted from the earlier paper [10].

The breaking stresses for unnotched PMMA specimens range from 7.0 Kg/mm<sup>2</sup> to 7.3 Kg/mm<sup>2</sup>.

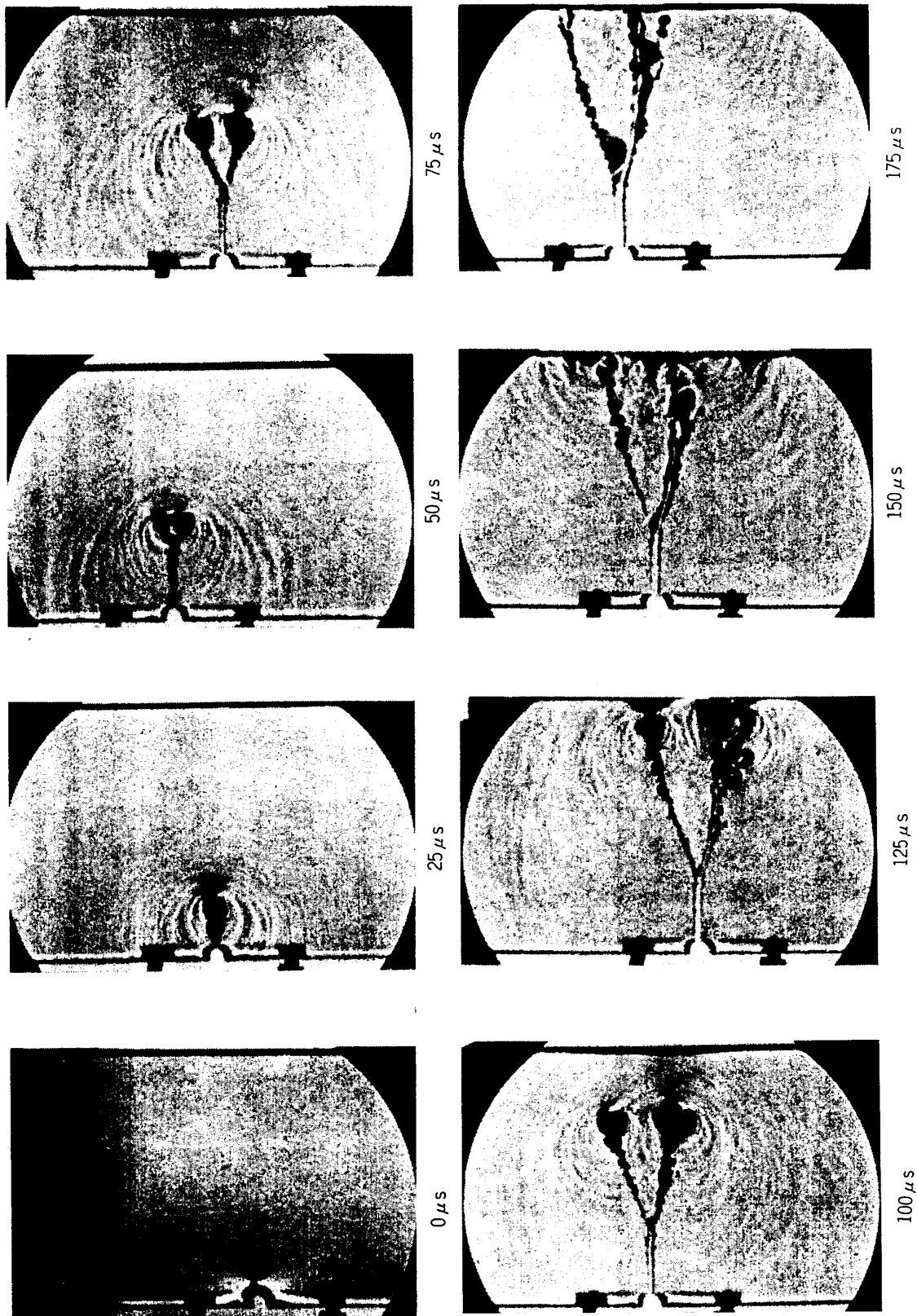
### ANALYSIS OF EXPERIMENTAL RESULTS

As seen from Figs. 5 to 7, the incident and reflected strain disturbances ahead of a running crack are distinctly observed through high speed Schlieren photography.

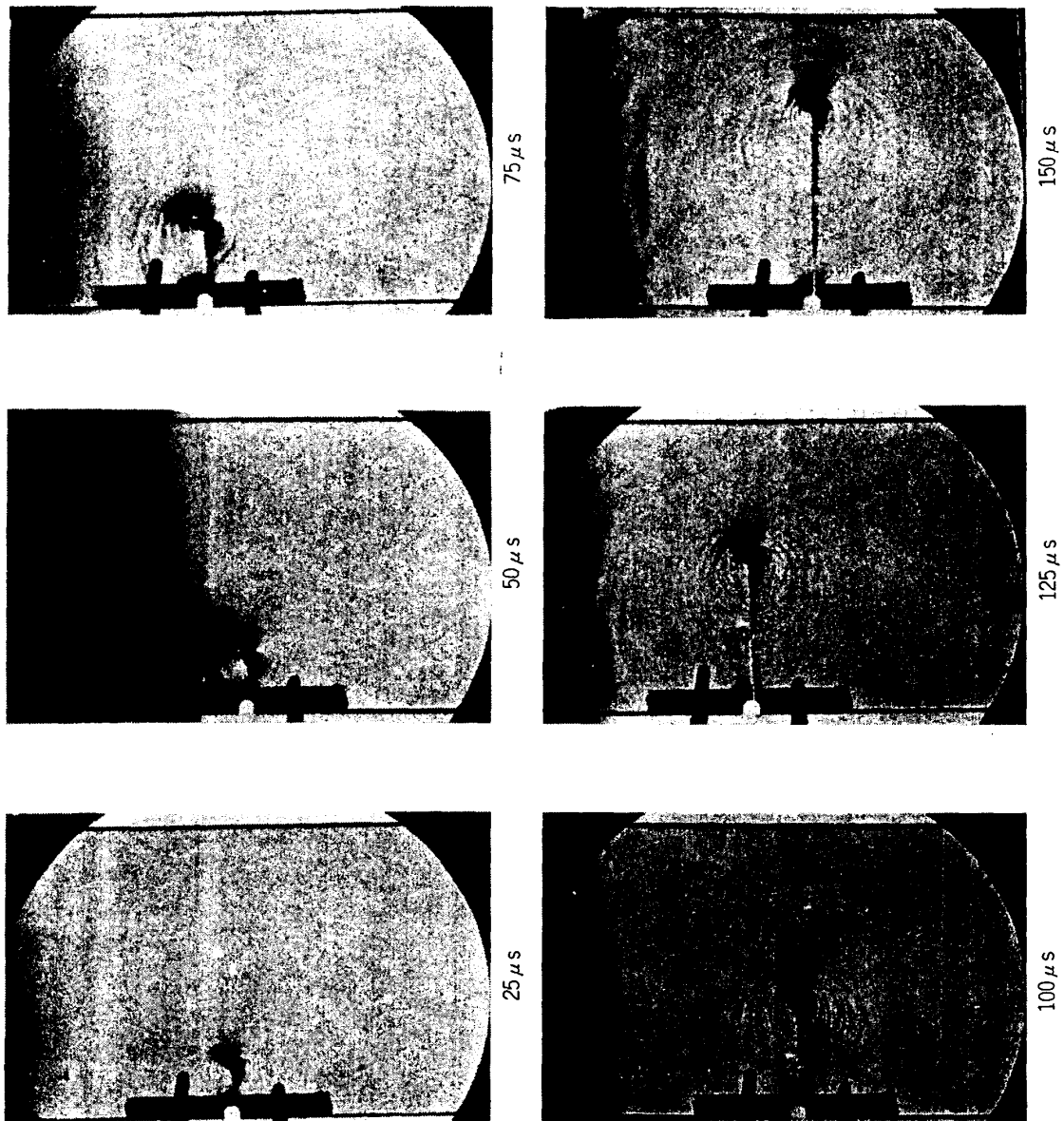
Although neither velocity gages nor strain gages are attached on the specimen surface in order not to hurt the surface optical calmness in taking Schlieren photographs, the crack propagation velocity realized in Figs. 5 to 7 would be estimated to be about 70% of theoretical crack velocity in elastic solids at best compared with the results obtained in the earlier paper [11], and the maximum surface strain disturbances could also be roughly estimated ranging from 0.03% to 0.1% according to the breaking stress and the applied strain rate as judged from the strain gage values of the previous results [12].

The observed wavy strain disturbance pattern is very interesting, because this might suggest that the dynamic crack propagation in such a viscoelastic solid would be of intermittent growth, and that the wavy pattern would presumably be produced each time a crack begins to start after very short interruption in its intermittent propagating process, which would be well conjectured from inspection of interval of fracture surface parabolic marking characteristic of PMMA [11]. That is, the strain disturbances due to the rapid growth of a crack propagate as compressive waves varying the local density in the viscoelastic solid, resulting in the change in the local refractive index, and thus producing such wavy pattern in the Schlieren photographs. From these observed Schlieren photographs, Figs. 5 to 7, the degree of wavy strain disturbances rather depends on the breaking stress, i.e., higher disturbances are observed for higher breaking stress, and the strain rate does almost no effects on the formation of wavy strain disturbances, as seen from Figs. 8 and 9.

In a viscoelastic solid, such wavy disturbances due to the compressive waves originating from rapid growth of a crack might be fully expected due to the fluid-like behavior attributed to inherent viscous element.

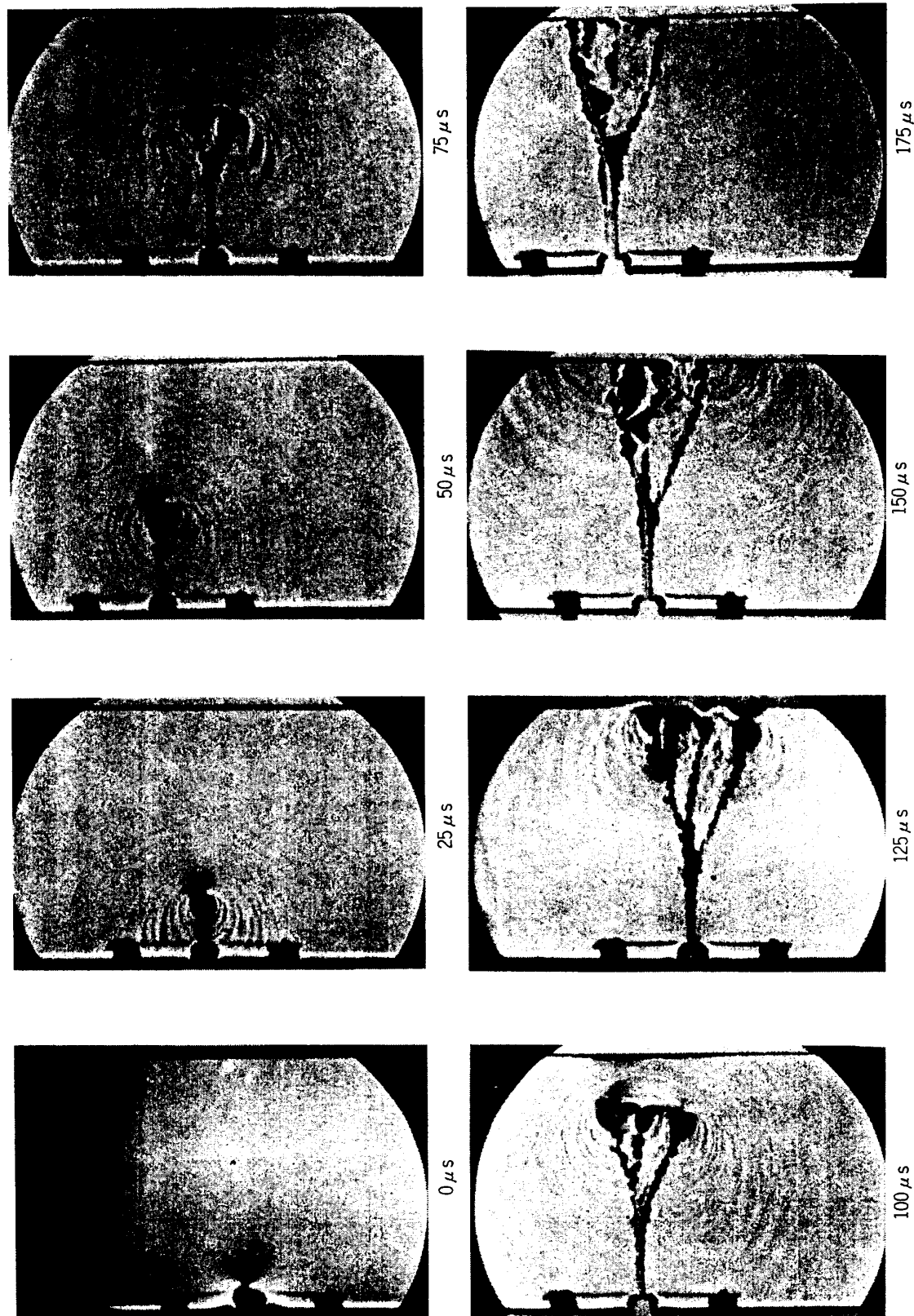


No. 3 ( $\rho = 2.5 \text{ mm}$ ,  $\dot{\epsilon} = 1.93 \times 10^{-2} \text{ s}^{-1}$ ,  $\sigma_0 = 3.6 \text{ kg/mm}^2$ )  
 FIG. 5 Schlieren photograph for No. 3 specimen



No. 13 ( $\rho = 0.02$  mm,  $\dot{\epsilon} = 7.93 \times 10^{-6} \text{ s}^{-1}$ ,  $\sigma_b = 1.8 \text{ kg/mm}^2$ )

FIG. 6 Schlieren photograph for No. 13 specimen



No. 14 ( $\rho = 2.5 \text{ mm}$ ,  $\epsilon = 7.93 \times 10^{-3} \text{ s}^{-1}$ ,  $\sigma_0 = 4.3 \text{ kg/mm}^2$ )  
FIG. 7 Schlieren photograph for No. 14 specimen

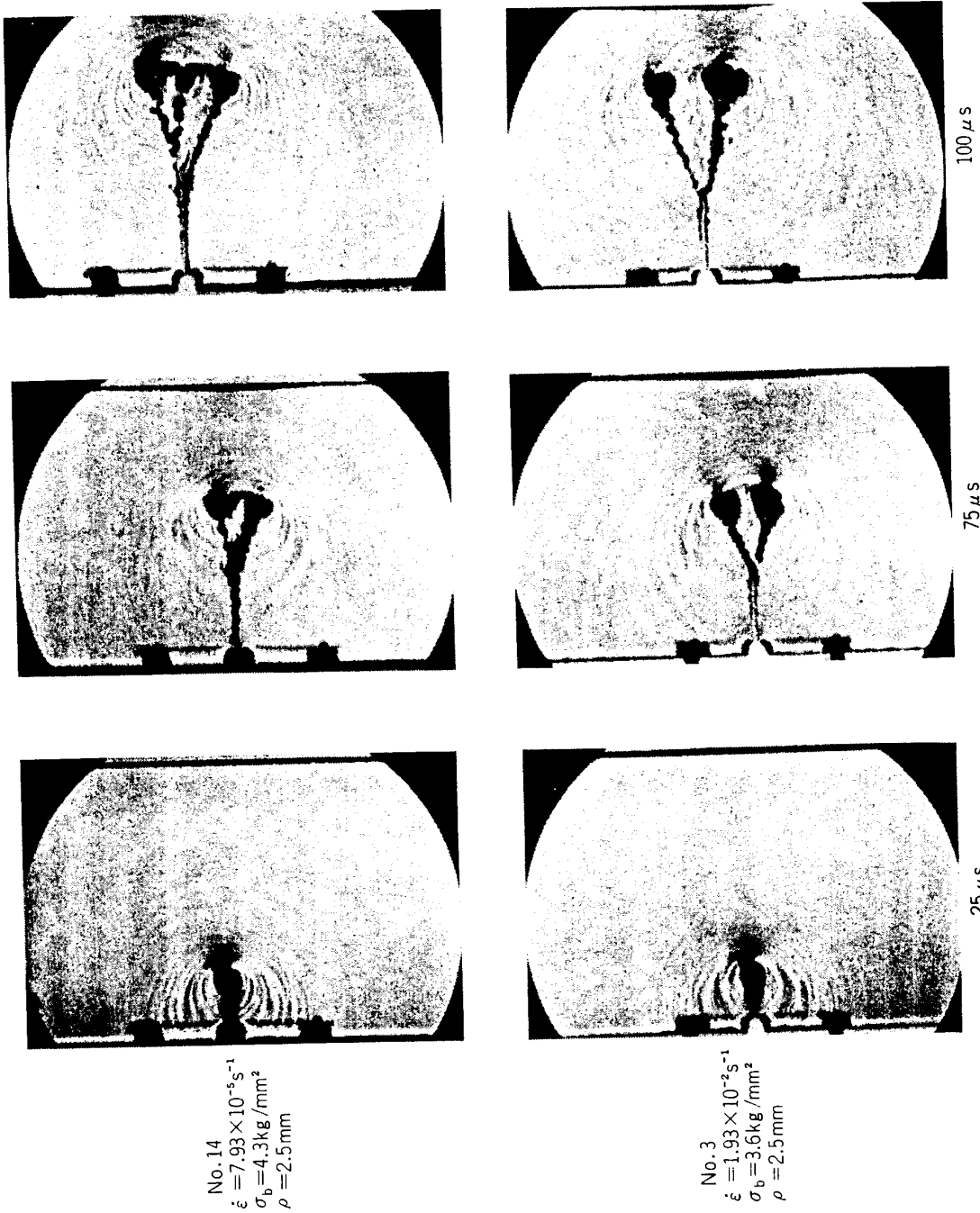
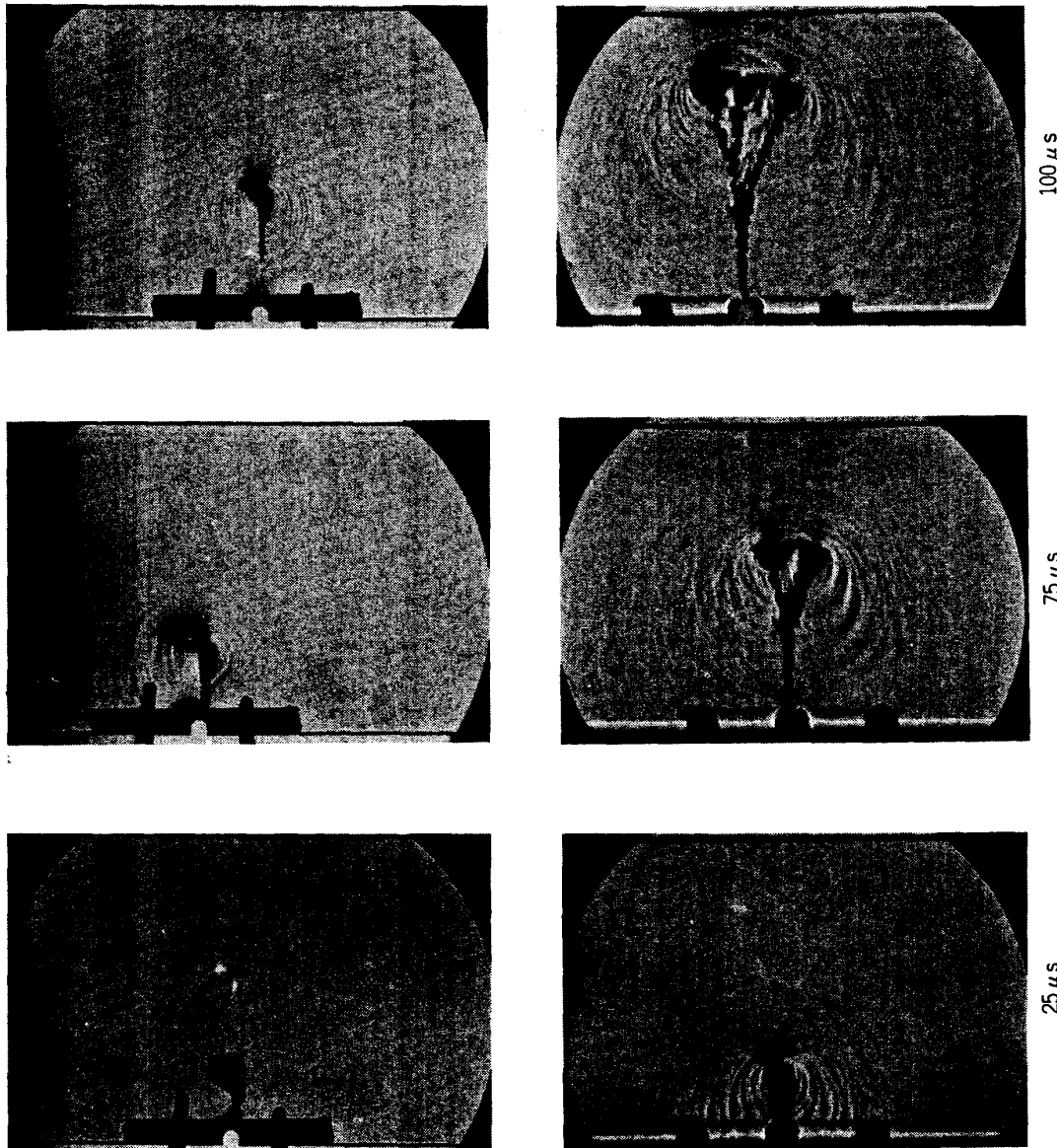


FIG. 8 Comparison of Schlieren Photographs (No. 3 vs. No. 14)



No. 13  
 $\rho = 0.02 \text{ mm}$   
 $\sigma_b = 1.8 \text{ kg/mm}^2$   
 $\dot{\epsilon} = 7.93 \times 10^{-6} \text{ s}^{-1}$

No. 14  
 $\rho = 2.5 \text{ mm}$   
 $\sigma_b = 4.3 \text{ kg/mm}^2$   
 $\dot{\epsilon} = 7.93 \times 10^{-6} \text{ s}^{-1}$

100  $\mu\text{s}$

75  $\mu\text{s}$

25  $\mu\text{s}$

FIG. 9 Comparison of Schlieren photographs (No. 13 vs. No. 14)

## CONCLUSIONS

The experimental study on the preceding strain disturbance ahead of a running crack in a viscoelastic solid during dynamic fracture was performed. Visual observation through Schlieren photographic techniques recognized the existence of preceding viscoelastic strain disturbances ahead of a running crack and revealed the general propagating wavy pattern of such preceding viscoelastic strain disturbances. It was observed that the breaking stress affects the degree of strain disturbances, i.e., the higher breaking stress much enhances strain disturbances and vice versa, while the applied strain rate to initiate a running crack contributes little effects on the disturbances so far as the present study is concerned. It is well conjectured that the observed wavy disturbance pattern might support the intermittent crack propagation phenomenon in such a viscoelastic solid. Further effort will be continued.

## ACKNOWLEDGEMENTS

The authors appreciate Professor Kozo Kawata for his encouragement. Mr. Tadashi Sato is also acknowledged for his help in performing experiment.

The present work was partly sponsored by Ministry of Education under grant in aid for scientific research.

*Department of Materials  
Institute of Space and Aeronautical Science  
University of Tokyo  
April 21, 1975*

## REFERENCES

- [ 1 ] J. Hopkinson, Original Papers Vol. 2, p. 316. Cambridge, London, 1872 (Published in 1901)
- [ 2 ] B. Hopkinson, Proc. R. Soc. A89, 411 (1914)
- [ 3 ] J. S. Rinehart & J. Pearson, Behavior of Metals under impulsive loads. ASM, Cleveland (1954)
- [ 4 ] H. Kolsky & D. Rader, Treatise on Fracture, Vol. 1, edited by H. Liebowitz, pp. 553-569, Academic Press (1968)
- [ 5 ] J. Miklowitz, J. Appl. Mech. 20, 122 (1952)
- [ 6 ] J. W. Phillips, Int' J. Solids & Structures, 6, 1403 (1970)
- [ 7 ] H. Kolsky & Y. M. Tsai, J. Mech. & Phys. Solids, 15, 263 (1967)
- [ 8 ] Y. M. Tsai, J. Mech. & Phys. Solids, 16, 133 (1968)
- [ 9 ] H. Kolsky, Engng. Fracture Mech. 5, 513 (1973)
- [ 10 ] A. Kobayashi & T. Sato, Bull. Inst. Space & Aero. Sci., Univ. of Tokyo, 10, 2(B), 311 (1974) (in Japanese)
- [ 11 ] A. Kobayashi, N. Ohtani & T. Sato, J. Appl. Polymer Sci., 18, 6, 1625 (1974)
- [ 12 ] A. Kobayashi & T. Sato, J. Appl. Polymer Sci., 18, 7, 2039 (1974)